JGP Journal of General Physiology

VIEWPOINT

Visualization of expanding fusion pores in secretory cells

Prabhodh S. Abbineni[1], Daniel Axelrod[1,2], and Ronald W. Holz[1]

Secretory cells package their protein cargo into granules, which must fuse with the plasma membrane for these proteins to be released. Such exocytosis requires not only fusion of the granule membrane with the plasma membrane but also expansion of the fusion pore from the earliest detectable diameter (2–3 nm) to tens of nanometers or more. New optical techniques have enabled live imaging of the expanding fusion pore and have revealed unexpected diversity and regulation of this last step of exocytosis. Indeed, a series of papers from the laboratory of Ling-Gang Wu have used elegant, live-cell confocal and 3-D stimulated emission depletion (STED)–based imaging techniques to examine secretory granules in chromaffin cells immediately before and after fusion. Using cytosolic leaflet probes, mainly GFP-tagged pleckstrin homology domain of phospholipase C δ1 (PH-GFP), which binds to phosphatidtylinositol 4,5 bisphosphate, this work has provided beautiful images of the omega figures indicative of fusion. In this article, we put these studies into an historical context and examine the dynamics and implications of fusion-induced accumulation of phosphatidylinositol 4,5-bisphosphate on the granule membrane. We also discuss diffusion of lipid-associated protein through the fusion pore.

Historical perspective

The classical studies of Palade revealed by electron microscopy omega figures that reflect protein discharge at the plasma membrane in pancreatic acinar cells (Palade, 1975). Early electron microscopic studies demonstrated a variety of configurations of the fused granule membrane in anterior pituitary cells (Farquhar, 1961), posterior pituitary cells (Nagasawa et al., 1970), and adrenal chromaffin cells (Grynszpan-Winograd, 1971). The development of rapid freezing techniques (Heuser et al., 1979) eliminated both spatial and temporal fixation artifacts that confounded earlier studies that imaged secreting cells. These techniques permitted the capture for the first time of virtually instantaneous images of fusion pores at varying degrees of expansion in mast cells (Chandler and Heuser, 1980; Curran et al., 1993), *Limulus* amoebocytes (Ornberg and Reese, 1981), and chromaffin cells (Schmidt et al., 1983). Investigations of the fusion pore in living cell (reviewed in Chang et al., 2017; Sharma and Lindau, 2018) began with the identification of a narrow, dynamic initial fusion pore using electrical techniques by the laboratories of Zimmerberg (Zimmerberg et al., 1987) and Almers (Breckenridge and Almers, 1987). In fact, electrical measurements demonstrated semistable fusion pores lasting for seconds from giant granules in mast cells of the beige mouse (Curran et al., 1993). Microamperometry, by measuring the kinetics of catecholamine discharge from individual secretory granules in chromaffin cells, provided further evidence for a narrow initial fusion pore (Chow et al., 1992; Jankowski et al., 1993; Albillos et al., 1997). Missing for many years was the real-time optical investigation of the transition from the narrow fusion pore to the longer-lived structures evident in electron micrographs. Such a structure was detected in living cells by imaging the cytosolic volume occupied by a fused granule (Taraska et al., 2003). Subsequently, high spatial and temporal resolution imaging capable of investigating a range of fusion outcomes was accomplished by measuring the orientation of a plasma membrane fluorophore (DiI), and thereby membrane curvature, using a combination of polarization and total internal reflection fluorescence microscopy (Anantharam et al., 2010). The diffusion of DiI from the plasma membrane into the granule membrane revealed the high-curvature, fused granule/plasma membrane interface. The approximate shape and dynamics of the structures could be inferred from the measurements and indicated a variety of outcomes. They ranged from a complete loss of curvature within 200 ms of fusion, consistent with collapse into the plasma membrane, to events in which curvature persisted for tens of seconds. The approach allowed direct investigation of the effects of the fusion pore on lumenal protein discharge. Importantly, the dynamics of the transition from the early fusion pore were found to be regulated by the GTPase

[1]Department of Pharmacology, University of Michigan Medical School, Ann Arbor, MI; [2]Department of Physics and LSA Biophysics, University of Michigan Medical School, Ann Arbor, MI.

Correspondence to Ronald W. Holz: holz@umich.edu.

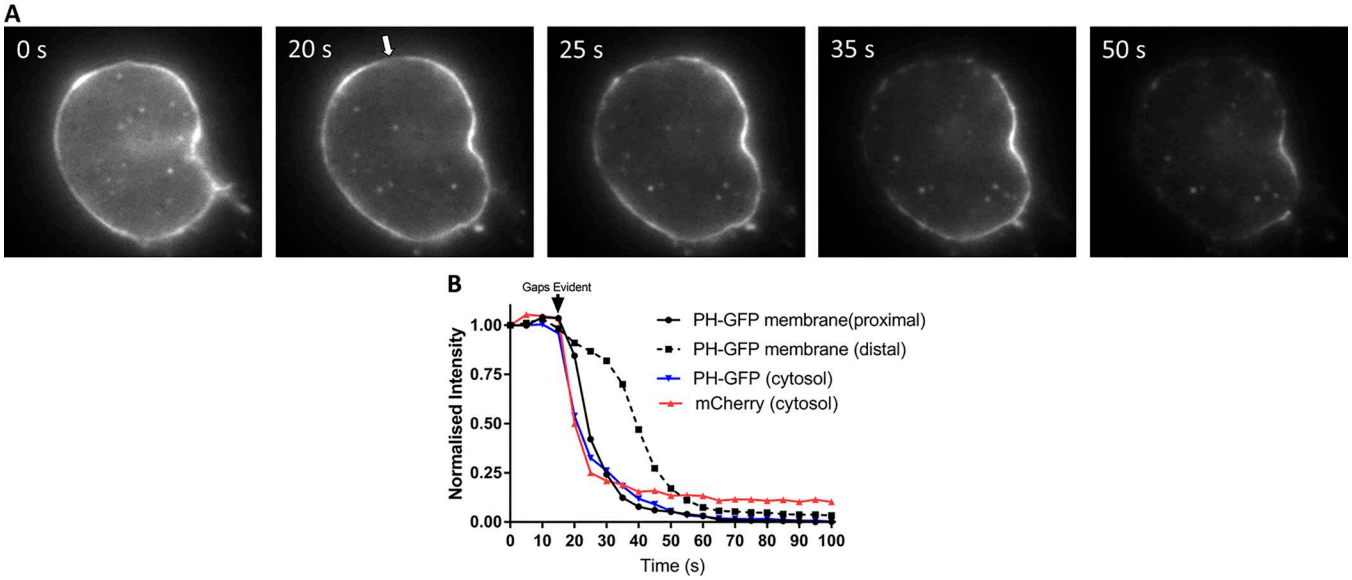

Figure 1. **Digitonin permeabilization reveals reversible binding of PH-GFP to the plasma membrane of chromaffin cells.** Bovine chromaffin cells were cotransfected with plasmids encoding PH-GFP and mCherry and imaged 5 d later in epifluorescence. Cells were bathed in Na glutamate solution (139 mM Na glutamate, 20 mM PIPES, 0.5 mM EGTA, 0.5 mM $MgCl_2$, and 2 mM ATP) at 27°C and individually perfused with bath solution containing 10 µM digitonin through a 100-µm-inner-diameter glass pipette. **(A)** Within 30 s of digitonin application, gaps appeared in the PH-GFP–labeled plasma membrane (arrow) and a wave of loss of membrane PH-GFP fluorescence occurred starting at the plasma membrane proximal to the gaps. **(B)** PH-GFP intensities of segments of the plasma membrane proximal and distal to the gaps and in the cytosol were measured. Cytosolic mCherry fluorescence is rapidly lost coincident with the appearance of a gap in the plasma membrane, and PH-GFP fluorescence on the plasma membrane proximal to the gap decreases almost as rapidly as cytosolic mCherry and cytosolic PH-GFP. These results are similar to those from three other cells in which an initial gap in the PH-GFP fluorescence was detected.

activity of dynamin (Anantharam et al., 2010, 2011), lumenal granule protein (Weiss et al., 2014), and synaptotagmin (Rao et al., 2014).

Live imaging of the expanding fusion pore

Recent work from Ling-Gang Wu and colleagues has used live-cell confocal and 3-D STED-based imaging techniques to examine secretory granules in chromaffin cells immediately before and after fusion (Zhao et al., 2016; Shin et al., 2018). In one study (Shin et al., 2018), the authors examined the fate of the granule after initial fusion pore formation and provided images of the omega figures associated with fusion. Fusion pores ranging from 60-nm diameter (the lateral resolution limit in 3-D STED) to >100 nm were often evident. Most of the experiments relied on a cytosolic leaflet probe for phosphatidylinositol 4,5-bisphosphate (PI-4,5-P_2), PH-GFP, although other membrane probes were also used.

This work by Shin et al. (2018) therefore confirms and extends current understanding that there are numerous fates of the secretory granule membrane after the formation of the initial narrow fusion pore (~2-nm diameter) and that fusion pore expansion can be regulated. What is significant and unique about the studies is the remarkable imaging that reveals the actual geometries of the postfusion granule membrane, with time resolution sometimes as short as 26 ms. The imaging directly demonstrates that the partially expanded fusion pore is dynamic. Note that one should cautiously interpret the details of the dynamics and relative frequencies of the various configurations of the postfusion granule membrane because imaging was performed at 20–22°C, not at 37°C. Membrane events associated with secretion are significantly temperature sensitive (Bittner and Holz, 1992; Earles et al., 2001; Micheva and Smith, 2005; Zhang and Jackson, 2008).

Use of PH-GFP to label cytosolic membrane leaflet

The authors interpret the labeling of the granule membrane by PH-GFP upon fusion (and often before fusion) as reflecting the diffusion of PH-GFP/PI-4,5-P_2 complex from the cytosolic leaflet of the plasma membrane into the fused cytosolic leaflet of the chromaffin granule. There are at least three issues to consider that are relevant for the interpretation of the experimental results with the probe: reversibility of binding, effects on exocytosis, and diffusion times into the fused granule membrane.

Dynamic binding of PH-GFP to membrane PI-4,5-P_2

The PH domain of phospholipase C δ_1 binds to PI-4,5-P_2 (and cytosolic IP_3) and was developed by the laboratory of T. Balla as a probe of PI-4,5-P_2–containing membranes (Várnai and Balla, 1998). Membrane-bound PH-GFP is in dynamic equilibrium with cytosolic PH-GFP and changes in the concentrations of PI-4,5-P_2 or IP_3 rapidly alter the equilibrium (Várnai and Balla, 1998). Studies in HEK cells examined quantitatively the dynamics of PH-GFP in the plasma membrane at 37°C (Hammond et al., 2009). The diffusion coefficient of PH-GFP when bound to PI-4,5-P_2 is ~10^{-8} cm^2/s. The probe dissociates from the plasma membrane with a time constant of 2 s. Association rates are much more rapid. The characteristic range of travel of membrane-bound PH-GFP before it dissociates from PI-4,5-P_2 is ~2 µm. It is likely that PH-GFP in chromaffin cells has similar dynamics. It dissociates within seconds from the plasma membrane not only upon activation of phospholipase C (Holz et al., 2000), but also upon plasma mem-

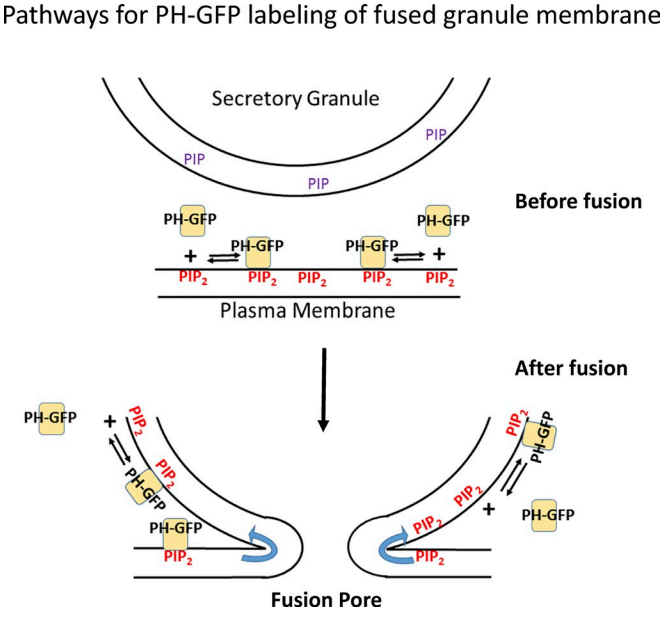

Figure 2. **Dynamic binding of PH-GFP and PI-4,5-P_2 and postfusion labeling of the secretory granule membrane.** PH-GFP reversibly binds to PI-4,5-P_2. The stable labeling of the fused granule membrane by PH-GFP probably reflects diffusion of PI-4,5-P_2, bound or unbound to PH-GFP, with simultaneous association and dissociation of PH-GFP and PI-4,5-P_2. The left and right side of the fusion pore depict diffusion of PH-GFP/PI-4,5-P_2 or unbound PI-4,5-P_2, respectively. De novo synthesis of PI-4,5-P_2 on the fused granule membrane (see text) would also enhance PH-GFP binding.

brane permeabilization with a low concentration of digitonin as shown in Fig. 1. Membrane-bound PH-GFP is lost from the membrane coincident with the loss of a cytosolic marker, mCherry (Fig. 1). Because fusion profiles imaged by PH-GFP have durations of many seconds (Zhao et al., 2016; Shin et al., 2018), the labeling undoubtedly reflects dynamic exchange of the probe between the membrane and cytosol as diagramed in Fig. 2. Importantly, the stable labeling with PH-GFP of the granule membrane upon fusion (and before fusion, see below) indicates that granule membrane has acquired PI-4,5-P_2.

PH-GFP inhibits exocytosis

An earlier study using this probe demonstrated in chromaffin cells that the plasma membrane, but not the secretory granule membrane, is labeled by PH-GFP, indicating that plasma membrane but not the secretory granule membrane before fusion contains PI-4,5-P_2 (Holz et al., 2000). Importantly, the study demonstrated that PH-GFP partially inhibits fusion over a wide range of Ca^{2+} currents, providing further support for a role of PI-4,5-P_2 in exocytosis, as shown by other studies (Eberhard et al., 1990; Hay and Martin, 1993; Hay et al., 1995; Milosevic et al., 2005). Fusion is likely compromised because PH-GFP competes with proteins that must bind to PI-4,5-P_2 to enable exocytosis. It is unknown whether changing the effective concentration of PI-4,5-P_2 at the fusion site changes only the probability of exocytosis or additionally alters fusion pore profiles and dynamics, an important issue for the interpretation of the optical experiments using PH-GFP (Zhao et al., 2016; Shin et al., 2018).

Diffusion times into the fused granule membrane

Labeling of the granule membrane with PH-GFP commences within tens of milliseconds of fusion (Shin et al., 2018), with a time constant of ∼400 ms (Zhao et al., 2016). These findings are consistent with another study that detected an increase in a PI-4,5-P_2 at fusion sites at the time of discharge using another PI-4,5-P_2 probe (Trexler et al., 2016). How then does one interpret the labeling of the granule membrane with PH-GFP in the experiments by Wu and colleagues? The authors suggest in this and a previous publication (Zhao et al., 2016) that the probe bound to PI-4,5-P_2 diffuses from the plasma membrane through the fusion pore into the granule membrane. It is interesting to quantitatively consider the possibility. This mathematically complex diffusion problem has been solved in the context of lipid diffusion after viral fusion (Rubin and Chen, 1990). Fortuitously, the solution can be applied to the diffusion of PH-GFP/PI-4,5-P_2 from the plasma membrane of a 10.5-µm-radius cell into a fused granule membrane with a radius of 150 nm (dimensions appropriate for chromaffin granules and chromaffin cells) via fusion pores of radii of 7.5, 15, and 30 nm. These numbers give the same values of the dimensionless parameter Dt/R^2 (where D is the diffusion coefficient, t is time, and R is the radius of the cell) included in Fig. 2 of Rubin and Chen (1990) and underlying the calculations in Table 1 of Rubin and Chen (1990). As discussed above, the diffusion coefficient of membrane-bound PH-GFP is 10^{-8} cm^2/s (Hammond et al., 2009), similar to that of PI-4,5-P_2 (Golebiewska et al., 2011). It is the same diffusion constant used by Rubin and Chen in their calculation. From rows 4–6 of Table 1 of Rubin and Chen (1990), the time for the diffusing species to reach one-half of its final concentration in the granule membrane for fusion pores of radii 7.5, 15, and 30 nm are 234, 180, and 126 ms, respectively. The decrease in $t_{1/2}$ with increasing fusion pore radius is expected because of the greater circumference through which the protein–lipid complex can diffuse.

The Rubin and Chen solution is exact but requires considerable computational power to extend to other fusion pore radii. As a quicker and simpler alternative, we have calculated the minimum time it would take for diffusional flow from a planar plasma membrane to supply a fused granule with enough molecules to attain a concentration of one half its final concentration. The calculation assumes that the fusion pore ring is a "perfect sink" that instantly and permanently transfers every molecule that hits it into the granule (Eq. 5.79 in Crank [1967]). The assumption understates the true transfer time because the ring is not actually a perfect sink: some molecules that hit it from the planar membrane do in fact return to the planar membrane, thereby slowing the net transfer rate. For $D = 10^{-8}$ cm^2/s (the diffusion coefficient of PH-GFP in the plasma membrane; Hammond et al., 2009), granule radius = 150 nm, and fusion pore radii variously set to 7.5, 15, and 30 nm, the lower bounds for planar diffusion are 199, 130, and 68 ms, respectively (Fig. 3 A). To this minimum diffusion time in the plane, another delay must be taken into account: the time it takes for molecules to diffuse around the surface of the spherical granule after they arrive at the fusion pore ring. This latter time can be calculated from an exact theory (Velez and Axelrod, 1988) for the case where all the molecules arrive at the fusion ring simultaneously (which they do not). Nevertheless, this spherical surface

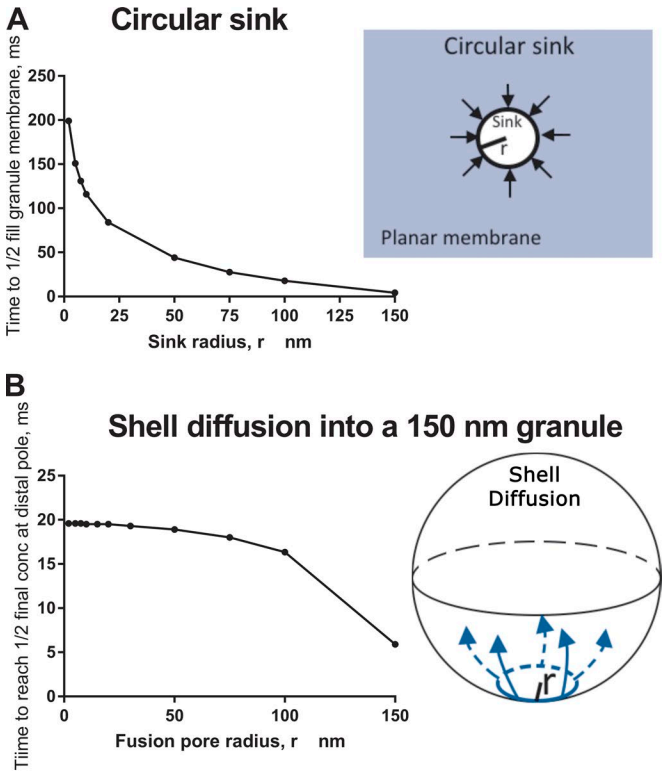

Figure 3. **Diffusion time for a lipid probe in the plasma membrane to accumulate in a fused secretory granule with a fusion pore.** The following calculations were performed with a diffusion constant of 1×10^{-8} cm^2/s for PH-GFP (Hammond et al., 2009). **(A)** Circular sink. Minimum time for diffusional flow from a planar plasma membrane to supply a fused granule with enough molecules to attain a concentration of one half its final concentration. The calculation from Eq. 5.79 in Crank (1967) assumes that the (fusion pore) ring is a "perfect sink" that instantly and permanently transfers every molecule that hits it into the granule. **(B)** Shell diffusion. Time to attain a concentration of one half the final concentration at the distal pole of a fused granule (300-nm diameter) if all of the protein that is to enter the granule is distributed at zero time along a ring (fusion pore) of specific radius. The calculation is based on Velez and Axelrod (1988). **(C)** Time to half fill the granule membrane with plasma membrane probe through the fusion pore. The exact solution to this complex diffusion pathway has been solved (Rubin and Chen, 1990). It was applied to the diffusion of PH-GFP/PI-4,5-P_2 from the plasma membrane of a 10.5-µm-radius cell into a fused granule membrane with a radius of 150 nm for fusion pores of radii of 7.5, 15, and 30 nm (red symbols). The three points were fitted with a parabola (red line), which was extrapolated to 2-nm pore radius (blue symbol and blue dashed line).The exact solution requires considerable computational power to extend to other fusion pore dimensions. Instead, the minimum time was estimated for a protein to reach one half of the final concentration by summing (black circles) the analyses in A and B. The minimum estimates of time and the exact solutions are remarkably consistent.

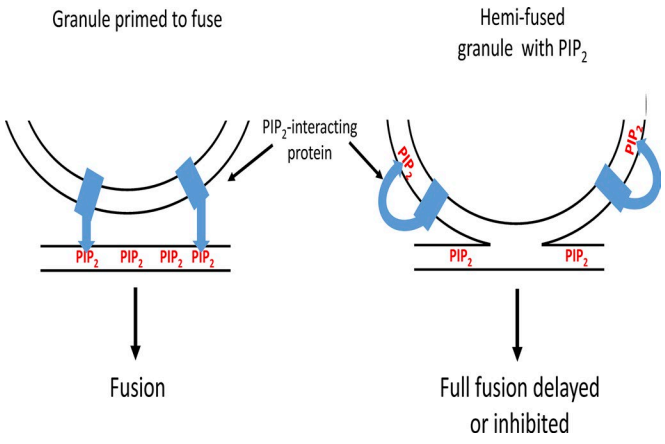

Figure 4. **Appearance of PI-4,5-P_2 on the granule membrane upon hemifusion may delay or inhibit full fusion by misdirecting PI-4,5-P_2–dependent reactions.** The functions of several proteins in the fusion pathway (e.g., synaptotagmin, CAPS, and Munc13) require binding to PI-4,5-P_2. It is generally thought that these interactions occur with plasma membrane PI-4,5-P_2. The functions of these proteins may be thwarted if the proteins interact with PI-4,5-P_2 on the granule membrane before full fusion. The cartoon illustrates how the membrane interaction of a granule protein such as synaptotagmin would be altered by the appearance of PI-4,5-P_2 in the granule membrane.

diffusion will only increase the total time needed for the granule to become populated. With the restricted assumption of a simultaneous start, the time needed for the distal pole of a spherical granule to reach 1/2 of its final concentration is ∼20 ms, decreasing only slightly with increasing fusion pore radius in the 2–30 nm range (Fig. 3 B). Therefore, from the relevant equations for the two steps, it is evident that the first step—diffusion from the plasma membrane through the fusion pore—is the rate-limiting step. The second step—diffusion around the spherical granule—adds only several tens of milliseconds to the whole process. The minimum time to approximately half fill the fused granule membrane is, very roughly, the sum of the calculations (Fig. 3 C, black symbols). The estimates of the minimal times for fusion pores of radii 7.5, 15, and 30 nm are consistent with the exact calculations (Fig. 3 C, red symbols). The Rubin and Chen exact results at their three values of pore size were fitted to a parabola (the lowest order polynomial that can pass through all three points), and the parabola was extrapolated to 2-nm pore size (blue symbol). The minimum time and the extrapolation were reasonably close, with the Rubin and Chen extrapolation being slower than the estimate as expected, because the Rubin and Chen (1990) calculation allows for back diffusion. For a stable initial fusion pore with an outer radius of 2 nm, the extrapolation estimates ∼300 ms to half fill the fused granule. These considerations also apply to unbound PI-4,5-P_2, which has a diffusion coefficient similar to that of PH-GFP/PI-4,5-P_2 as well as other lipid-based probes (Zhao et al., 2016).

The calculations indicate that for fusion pores that expand from radii of ∼2 to 30 nm, as in events imaged by Shin et al. (2018), the diffusion time of PH-GFP/PI-4,5-P_2 or PI-4,5-P_2 is 150–300 ms. Thus, the 400-ms time constant for labeling of newly fused granules by PH-GFP (Zhao et al., 2016) is consistent with diffusion of the probe bound to PI-4,5-P_2 or diffusion of the lipid alone with subsequent rapid binding of cytosolic PH-GFP. The calculations in addition reveal that diffusion into the fused

granule does not occur within milliseconds, but is relatively slow, leaving ample time for another pathway to populate the fused granule membrane with PI-4,5-P_2, which we consider below.

It should be noted that bulk movement of lipid by convection into or out of the fused granule membrane may occur if the fusion pore connects membranes at different tensions (Monck et al., 1990; Chizmadzhev et al., 1999). Lipid convection could account for the enlargement or shrinkage of postfusion granule profiles that have been observed by Wu and colleagues in chromaffin cells (Chiang et al., 2014). Lipid convection would either speed or retard the flux of PH-GFP/PI-4,5-P_2 into the granule membrane depending on the direction of convection.

Synthesis of PI-4,5-P_2 on the fused secretory granule membrane?

De novo synthesis of PI-4,5-P_2 on the granule membrane, in addition to diffusion, could contribute to the labeling of the granule membrane (cytosolic PH-GFP would then bind). PIP kinase I is associated with the plasma membrane (Choi et al., 2015). The chromaffin granule membrane contains PI-4-P (Hawthorne et al., 1980). The close association of the granule membrane to the plasma membrane upon or before fusion, by bringing the substrate and enzyme together, could stimulate PI-4,5-P_2 synthesis. There is, in fact, experimental support for the synthesis pathway. Direct biochemical measurements indicate that in both intact and permeabilized chromaffin cells, total cellular PI-4,5-P_2 increases by 10–30% in a Ca^{2+}-dependent manner (Eberhard and Holz, 1991) coincident with secretion. The increase in permeabilized cells occurs over the same range of Ca^{2+} concentrations (1–10 μM) that stimulates secretion, making it plausible that synthesis occurs on the newly fused granule membranes that significantly increase plasma membrane area. Indeed, the increase in surface area caused by fused granules during the biochemical experiments can be estimated to be ∼50% (assuming 10% of the granules undergoing exocytosis, a typical response in biochemical experiments), which is comparable to the increase in PI-4,5-P_2. The biochemical experiments had a time scale of minutes and represent the ensemble of biochemical reactions in the cell culture occurring as fusion occurs asynchronously in cells over many minutes upon global stimulation of the cultures. The synthesis of PI-4,5-P_2 at individual fusion sites would undoubtedly have much faster kinetics. We therefore propose that that labeling of the granule membrane by PH-GFP reflects, at least in part, synthesis of PI-4,5-P_2 on the fused granule membrane.

Implications of rapid PI-4,5-P_2 appearance on the fused granule membrane

Whatever the source of the lipid, the Shin et al. (2018) paper demonstrates that within tens of milliseconds of fusion, the granule membrane begins to acquire PI-4,5-P_2. The appearance of PI-4,5-P_2 on the granule membrane has overlooked functional implications. The fused granule membrane remains a distinct entity in the plasma membrane for many seconds to minutes and serves as a nucleation site for endocytosis (Ceridono et al., 2011; Bittner et al., 2013). Increased PI-4,5-P_2 on the fused membrane likely catalyzes PI-4,5-P_2–dependent protein reactions, including those of dynamin and clathrin adaptors that determine the fate of the fused granule membrane by two forms of endocytosis: (1) the binding of dynamin and the initiation within seconds of clathrin-independent endocytosis (fusion pore closure) (Artalejo et al., 1995, 2002; Elhamdani et al., 2006; Fulop et al., 2008), and (2) slower clathrin-mediated endocytosis that gradually internalizes via nibbling the granule membrane (Bittner et al., 2013).

There could be additional effects of PI-4,5-P_2 on the granule membrane. In ∼40% of the events, PH-GFP appears on the granule membrane before fusion or without subsequent fusion (Zhao et al., 2016). These events are relatively long-lived, often lasting for many seconds, and must reflect the appearance of PI-4,5-P_2 on the cytosolic leaflet of the granule membrane, through either diffusion or de novo PI-4,5-P_2 synthesis when the granule and plasma membrane are in close apposition before fusion. The functions of synaptotagmin (Bai et al., 2004), the Ca^{2+} sensor in the granule membrane, and the priming factors CAPS (Grishanin et al., 2004) and Munc13 (Shin et al., 2010; Kabachinski et al., 2014) all require interaction with PI-4,5-P_2. It is generally thought that the interaction occurs with plasma membrane PI-4,5-P_2. The functions of these proteins may be altered if the proteins interact with PI-4,5-P_2 on the granule membrane before full fusion (Fig. 4). Therefore, the proposed hemifusion profiles that were detected could represent slowed or thwarted fusion events as PI-4,5-P_2–dependent synaptotagmin, CAPS, or Munc13 interactions are misdirected to the granule membrane.

Summary and outlook

The recent studies by Wu and colleagues (Zhao et al., 2016; Shin et al., 2018) demonstrate the power of state-of-the-art imaging to illuminate and investigate rapid, nanoscale events at the plasma membrane. The studies raise numerous issues concerning consequences of the close apposition of the granule and plasma membrane before and during fusion. It is likely that there are pathways of labeling the fused granule membrane with PH-GFP in addition to diffusion PH-GFP/PI-4,5-P_2 complex from the cytosolic leaflet of the plasma membrane. Whatever the pathways for labeling, the studies unexpectedly reveal the remarkably rapid appearance of PI-4,5-P_2 on the granule membrane upon fusion, and sometimes before fusion pore formation. The immediate consequences of its appearance are unknown but undoubtedly reflect the central role of this lipid in exocytosis and its aftermath.

Acknowledgments

We thank Drs. Kevin P. Bohannon and Mary A. Bittner for many helpful discussions.

This work was supported by National Institutes of Health grant R01-170553 to R.W. Holz and D. Axelrod.

The authors declare no competing financial interests.

Author contributions: P.S. Abbineni performed experiments and helped conceive and write the Viewpoint. D. Axelrod performed the diffusion analysis and contributed to the writing of the Viewpoint. R.W. Holz helped conceive and write the Viewpoint and performed some of the calculations.

Lesley C. Anson served as editor.

Submitted: 24 July 2018
Accepted: 6 November 2018

References

Albillos, A., G. Dernick, H. Horstmann, W. Almers, G. Alvarez de Toledo, and M. Lindau. 1997. The exocytotic event in chromaffin cells revealed by patch amperometry. *Nature.* 389:509–512. https://doi.org/10.1038/39081

Anantharam, A., B. Onoa, R.H. Edwards, R.W. Holz, and D. Axelrod. 2010. Localized topological changes of the plasma membrane upon exocytosis visualized by polarized TIRFM. *J. Cell Biol.* 188:415–428. https://doi.org/10.1083/jcb.200908010

Anantharam, A., M.A. Bittner, R.L. Aikman, E.L. Stuenkel, S.L. Schmid, D. Axelrod, and R.W. Holz. 2011. A new role for the dynamin GTPase in the regulation of fusion pore expansion. *Mol. Biol. Cell.* 22:1907–1918. https://doi.org/10.1091/mbc.e11-02-0101

Artalejo, C.R., J.R. Henley, M.A. McNiven, and H.C. Palfrey. 1995. Rapid endocytosis coupled to exocytosis in adrenal chromaffin cells involves Ca2+, GTP, and dynamin but not clathrin. *Proc. Natl. Acad. Sci. USA.* 92:8328–8332. https://doi.org/10.1073/pnas.92.18.8328

Artalejo, C.R., A. Elhamdani, and H.C. Palfrey. 2002. Sustained stimulation shifts the mechanism of endocytosis from dynamin-1-dependent rapid endocytosis to clathrin- and dynamin-2-mediated slow endocytosis in chromaffin cells. *Proc. Natl. Acad. Sci. USA.* 99:6358–6363. https://doi.org/10.1073/pnas.082658499

Bai, J., W.C. Tucker, and E.R. Chapman. 2004. PIP2 increases the speed of response of synaptotagmin and steers its membrane-penetration activity toward the plasma membrane. *Nat. Struct. Mol. Biol.* 11:36–44. https://doi.org/10.1038/nsmb709

Bittner, M.A., and R.W. Holz. 1992. A temperature-sensitive step in exocytosis. *J. Biol. Chem.* 267:16226–16229.

Bittner, M.A., R.L. Aikman, and R.W. Holz. 2013. A nibbling mechanism for clathrin-mediated retrieval of secretory granule membrane after exocytosis. *J. Biol. Chem.* 288:9177–9188. https://doi.org/10.1074/jbc.M113.450361

Breckenridge, L.J., and W. Almers. 1987. Currents through the fusion pore that forms during exocytosis of a secretory vesicle. *Nature.* 328:814–817. https://doi.org/10.1038/328814a0

Ceridono, M., S. Ory, F. Momboisse, S. Chasserot-Golaz, S. Houy, V. Calco, A.M. Haeberlé, V. Demais, Y. Bailly, M.F. Bader, and S. Gasman. 2011. Selective recapture of secretory granule components after full collapse exocytosis in neuroendocrine chromaffin cells. *Traffic.* 12:72–88. https://doi.org/10.1111/j.1600-0854.2010.01125.x

Chandler, D.E., and J.E. Heuser. 1980. Arrest of membrane fusion events in mast cells by quick-freezing. *J. Cell Biol.* 86:666–674. https://doi.org/10.1083/jcb.86.2.666

Chang, C.W., C.W. Chiang, and M.B. Jackson. 2017. Fusion pores and their control of neurotransmitter and hormone release. *J. Gen. Physiol.* 149:301–322. https://doi.org/10.1085/jgp.201611724

Chiang, H.C., W. Shin, W.D. Zhao, E. Hamid, J. Sheng, M. Baydyuk, P.J. Wen, A. Jin, F. Momboisse, and L.G. Wu. 2014. Post-fusion structural changes and their roles in exocytosis and endocytosis of dense-core vesicles. *Nat. Commun.* 5:3356. https://doi.org/10.1038/ncomms4356

Chizmadzhev, Y.A., D.A. Kumenko, P.I. Kuzmin, L.V. Chernomordik, J. Zimmerberg, and F.S. Cohen. 1999. Lipid flow through fusion pores connecting membranes of different tensions. *Biophys. J.* 76:2951–2965. https://doi.org/10.1016/S0006-3495(99)77450-3

Choi, S., N. Thapa, X. Tan, A.C. Hedman, and R.A. Anderson. 2015. PIP kinases define PI4,5P_2 signaling specificity by association with effectors. *Biochim. Biophys. Acta.* 1851:711–723. https://doi.org/10.1016/j.bbalip.2015.01.009

Chow, R.H., L. von Rüden, and E. Neher. 1992. Delay in vesicle fusion revealed by electrochemical monitoring of single secretory events in adrenal chromaffin cells. *Nature.* 356:60–63. https://doi.org/10.1038/356060a0

Crank, J. 1967. The Mathematics of Diffusion. Oxford University Press, London.

Curran, M.J., F.S. Cohen, D.E. Chandler, P.J. Munson, and J. Zimmerberg. 1993. Exocytotic fusion pores exhibit semi-stable states. *J. Membr. Biol.* 133:61–75. https://doi.org/10.1007/BF00231878

Earles, C.A., J. Bai, P. Wang, and E.R. Chapman. 2001. The tandem C2 domains of synaptotagmin contain redundant Ca^{2+} binding sites that cooperate to engage t-SNAREs and trigger exocytosis. *J. Cell Biol.* 154:1117–1124. https://doi.org/10.1083/jcb.200105020

Eberhard, D.A., and R.W. Holz. 1991. Calcium promotes the accumulation of polyphosphoinositides in intact and permeabilized bovine adrenal chromaffin cells. *Cell. Mol. Neurobiol.* 11:357–370. https://doi.org/10.1007/BF00713279

Eberhard, D.A., C.L. Cooper, M.G. Low, and R.W. Holz. 1990. Evidence that the inositol phospholipids are necessary for exocytosis. Loss of inositol phospholipids and inhibition of secretion in permeabilized cells caused by a bacterial phospholipase C and removal of ATP. *Biochem. J.* 268:15–25. https://doi.org/10.1042/bj2680015

Elhamdani, A., F. Azizi, and C.R. Artalejo. 2006. Double patch clamp reveals that transient fusion (kiss-and-run) is a major mechanism of secretion in calf adrenal chromaffin cells: high calcium shifts the mechanism from kiss-and-run to complete fusion. *J. Neurosci.* 26:3030–3036. https://doi.org/10.1523/JNEUROSCI.5275-05.2006

Farquhar, M.G. 1961. Origin and fate of secretory granules in cells of the anterior pituitary gland. *Trans. N. Y. Acad. Sci.* 23(4 Series II):346–351. https://doi.org/10.1111/j.2164-0947.1961.tb01361.x

Fulop, T., B. Doreian, and C. Smith. 2008. Dynamin I plays dual roles in the activity-dependent shift in exocytic mode in mouse adrenal chromaffin cells. *Arch. Biochem. Biophys.* 477:146–154. https://doi.org/10.1016/j.abb.2008.04.039

Golebiewska, U., J.G. Kay, T. Masters, S. Grinstein, W. Im, R.W. Pastor, S. Scarlata, and S. McLaughlin. 2011. Evidence for a fence that impedes the diffusion of phosphatidylinositol 4,5-bisphosphate out of the forming phagosomes of macrophages. *Mol. Biol. Cell.* 22:3498–3507. https://doi.org/10.1091/mbc.e11-02-0114

Grishanin, R.N., J.A. Kowalchyk, V.A. Klenchin, K. Ann, C.A. Earles, E.R. Chapman, R.R. Gerona, and T.F. Martin. 2004. CAPS acts at a prefusion step in dense-core vesicle exocytosis as a PIP2 binding protein. *Neuron.* 43:551–562. https://doi.org/10.1016/j.neuron.2004.07.028

Grynszpan-Winograd, O. 1971. Morphological aspects of exocytosin in the adrenal medulla. *Philos. Trans. R. Soc. Lond. B Biol. Sci.* 261:291–292. https://doi.org/10.1098/rstb.1971.0058

Hammond, G.R.V., Y. Sim, L. Lagnado, and R.F. Irvine. 2009. Reversible binding and rapid diffusion of proteins in complex with inositol lipids serves to coordinate free movement with spatial information. *J. Cell Biol.* 184:297–308. https://doi.org/10.1083/jcb.200809073

Hawthorne, J.N., N. Mohd, A. Lymberopoulos, and G. Lymberopoulos. 1980. Membrane phospholipids, exocytosis and cell division. *Biochem. Soc. Trans.* 8:30–32. https://doi.org/10.1042/bst0080030

Hay, J.C., and T.F. Martin. 1993. Phosphatidylinositol transfer protein required for ATP-dependent priming of Ca(2+)-activated secretion. *Nature.* 366:572–575. https://doi.org/10.1038/366572a0

Hay, J.C., P.L. Fisette, G.H. Jenkins, K. Fukami, T. Takenawa, R.A. Anderson, and T.F. Martin. 1995. ATP-dependent inositide phosphorylation required for Ca(2+)-activated secretion. *Nature.* 374:173–177. https://doi.org/10.1038/374173a0

Heuser, J.E., T.S. Reese, M.J. Dennis, Y. Jan, L. Jan, and L. Evans. 1979. Synaptic vesicle exocytosis captured by quick freezing and correlated with quantal transmitter release. *J. Cell Biol.* 81:275–300. https://doi.org/10.1083/jcb.81.2.275

Holz, R.W., M.D. Hlubek, S.D. Sorensen, S.K. Fisher, T. Balla, S. Ozaki, G.D. Prestwich, E.L. Stuenkel, and M.A. Bittner. 2000. A pleckstrin homology domain specific for phosphatidylinositol 4, 5-bisphosphate (PtdIns-4,5-P2) and fused to green fluorescent protein identifies plasma membrane PtdIns-4,5-P2 as being important in exocytosis. *J. Biol. Chem.* 275:17878–17885. https://doi.org/10.1074/jbc.M000925200

Jankowski, J.A., T.J. Schroeder, E.L. Ciolkowski, and R.M. Wightman. 1993. Temporal characteristics of quantal secretion of catecholamines from adrenal medullary cells. *J. Biol. Chem.* 268:14694–14700.

Kabachinski, G., M. Yamaga, D.M. Kielar-Grevstad, S. Bruinsma, and T.F. Martin. 2014. CAPS and Munc13 utilize distinct PIP2-linked mechanisms to promote vesicle exocytosis. *Mol. Biol. Cell.* 25:508–521. https://doi.org/10.1091/mbc.e12-11-0829

Micheva, K.D., and S.J. Smith. 2005. Strong effects of subphysiological temperature on the function and plasticity of mammalian presynaptic terminals. *J. Neurosci.* 25:7481–7488. https://doi.org/10.1523/JNEUROSCI.1801-05.2005

Milosevic, I., J.B. Sørensen, T. Lang, M. Krauss, G. Nagy, V. Haucke, R. Jahn, and E. Neher. 2005. Plasmalemmal phosphatidylinositol-4,5-bisphosphate level regulates the releasable vesicle pool size in chromaffin cells. *J. Neurosci.* 25:2557–2565. https://doi.org/10.1523/JNEUROSCI.3761-04.2005

Monck, J.R., G. Alvarez de Toledo, and J.M. Fernandez. 1990. Tension in secretory granule membranes causes extensive membrane transfer through the exocytotic fusion pore. *Proc. Natl. Acad. Sci. USA.* 87:7804–7808. https://doi.org/10.1073/pnas.87.20.7804

Nagasawa, J., W.W. Douglas, and R.A. Schulz. 1970. Ultrastructural evidence of secretion by exocytosis and of "synaptic vesicle" formation in pos-

terior pituitary glands. *Nature.* 227:407–409. https://doi.org/10.1038/227407a0

Ornberg, R.L., and T.S. Reese. 1981. Beginning of exocytosis captured by rapid-freezing of Limulus amebocytes. *J. Cell Biol.* 90:40–54. https://doi.org/10.1083/jcb.90.1.40

Palade, G. 1975. Intracellular aspects of the process of protein synthesis. *Science.* 189:867. https://doi.org/10.1126/science.189.4206.867-b

Rao, T.C., D.R. Passmore, A.R. Peleman, M. Das, E.R. Chapman, and A. Anantharam. 2014. Distinct fusion properties of synaptotagmin-1 and synaptotagmin-7 bearing dense core granules. *Mol. Biol. Cell.* 25:2416–2427. https://doi.org/10.1091/mbc.e14-02-0702

Rubin, R.J., and Y.D. Chen. 1990. Diffusion and redistribution of lipid-like molecules between membranes in virus-cell and cell-cell fusion systems. *Biophys. J.* 58:1157–1167. https://doi.org/10.1016/S0006-3495(90)82457-7

Schmidt, W., A. Patzak, G. Lingg, H. Winkler, and H. Plattner. 1983. Membrane events in adrenal chromaffin cells during exocytosis: a freeze-etching analysis after rapid cryofixation. *Eur. J. Cell Biol.* 32:31–37.

Sharma, S., and M. Lindau. 2018. The fusion pore, 60 years after the first cartoon. *FEBS Lett.* 592:3542–3562. https://doi.org/10.1002/1873-3468.13160

Shin, O.H., J. Lu, J.S. Rhee, D.R. Tomchick, Z.P. Pang, S.M. Wojcik, M. Camacho-Perez, N. Brose, M. Machius, J. Rizo, et al. 2010. Munc13 C2B domain is an activity-dependent Ca2+ regulator of synaptic exocytosis. *Nat. Struct. Mol. Biol.* 17:280–288. https://doi.org/10.1038/nsmb.1758

Shin, W., L. Ge, G. Arpino, S.A. Villarreal, E. Hamid, H. Liu, W.D. Zhao, P.J. Wen, H.C. Chiang, and L.G. Wu. 2018. Visualization of membrane pore in live cells reveals a dynamic-pore theory governing fusion and endocytosis. *Cell.* 173:934–945.e12. https://doi.org/10.1016/j.cell.2018.02.062

Taraska, J.W., D. Perrais, M. Ohara-Imaizumi, S. Nagamatsu, and W. Almers. 2003. Secretory granules are recaptured largely intact after stimulated exocytosis in cultured endocrine cells. *Proc. Natl. Acad. Sci. USA.* 100:2070–2075. https://doi.org/10.1073/pnas.0337526100

Trexler, A.J., K.A. Sochacki, and J.W. Taraska. 2016. Imaging the recruitment and loss of proteins and lipids at single sites of calcium-triggered exocytosis. *Mol. Biol. Cell.* 27:2423–2434. https://doi.org/10.1091/mbc.e16-01-0057

Várnai, P., and T. Balla. 1998. Visualization of phosphoinositides that bind pleckstrin homology domains: calcium- and agonist-induced dynamic changes and relationship to myo-[3H]inositol-labeled phosphoinositide pools. *J. Cell Biol.* 143:501–510. https://doi.org/10.1083/jcb.143.2.501

Velez, M., and D. Axelrod. 1988. Polarized fluorescence photobleaching recovery for measuring rotational diffusion in solutions and membranes. *Biophys. J.* 53:575–591. https://doi.org/10.1016/S0006-3495(88)83137-0

Weiss, A.N., A. Anantharam, M.A. Bittner, D. Axelrod, and R.W. Holz. 2014. Lumenal protein within secretory granules affects fusion pore expansion. *Biophys. J.* 107:26–33. https://doi.org/10.1016/j.bpj.2014.04.064

Zhang, Z., and M.B. Jackson. 2008. Temperature dependence of fusion kinetics and fusion pores in Ca2+-triggered exocytosis from PC12 cells. *J. Gen. Physiol.* 131:117–124. https://doi.org/10.1085/jgp.200709891

Zhao, W.D., E. Hamid, W. Shin, P.J. Wen, E.S. Krystofiak, S.A. Villarreal, H.C. Chiang, B. Kachar, and L.G. Wu. 2016. Hemi-fused structure mediates and controls fusion and fission in live cells. *Nature.* 534:548–552. https://doi.org/10.1038/nature18598

Zimmerberg, J., M. Curran, F.S. Cohen, and M. Brodwick. 1987. Simultaneous electrical and optical measurements show that membrane fusion precedes secretory granule swelling during exocytosis of beige mouse mast cells. *Proc. Natl. Acad. Sci. USA.* 84:1585–1589. https://doi.org/10.1073/pnas.84.6.1585